Geophysical Research Letters

RESEARCH LETTER
10.1029/2023GL103415

Nature and Origin of Magnetic Lineations Within Valdivia Bank: Ocean Plateau Formation by Complex Seafloor Spreading

S. Thoram[1], W. W. Sager[1], K. Gaastra[2], S. M. Tikoo[3,4], C. Carvallo[5], A. Avery[6], Arianna V. Del Gaudio[7], Y. Huang[8], K. Hoernle[9], T. W. Höfig[10,11], R. Bhutani[12], D. M. Buchs[13], C. Class[14], Y. Dai[15], G. Dalla Valle[16], S. Fielding[17], S. Han[18], D. E. Heaton[19], S. Homrighausen[9], Y. Kubota[20], C.-F. Li[21], W. R. Nelson[22], E. Petrou[23], K. E. Potter[24], S. Pujatti[25], J. Scholpp[26], J. W. Shervais[24], M. Tshiningayamwe[27], X. J. Wang[28], and M. Widdowson[29]

[1]Department of Earth and Atmospheric Sciences, University of Houston, Houston, TX, USA, [2]Department of Earth, Environmental and Planetary Sciences, Rice University, Houston, TX, USA, [3]Department of Geophysics, Stanford University, Stanford, CA, USA, [4]Department of Geological Sciences, Stanford University, Stanford, CA, USA, [5]Sorbonne Université, MNHN, CNRS, UMR, Institut de Minéralogie, de Physique des Matériaux et de Cosmochimie, Paris, France, [6]School of Geosciences, University of South Florida, Tampa, FL, USA, [7]Institute of Earth Sciences, University of Graz, Graz, Austria, [8]Key Laboratory of Exploration Technologies for Oil and Gas Resources (Yangtze University), Ministry of Education, Wuhan, China, [9]GEOMAR Helmholtz Centre for Ocean Research Kiel, Kiel, Germany, [10]International Ocean Discovery Program, Texas A&M University, College Station, TX, USA, [11]Coastal, Marine, and Polar Research, Jülich Research Centre (FZJ) Rostock, Jülich, Germany, [12]Department of Earth Sciences, Pondicherry University, Puducherry, India, [13]School of Earth and Ocean Sciences, Cardiff University, Cardiff, UK, [14]Lamont-Doherty Earth Observatory, Columbia University, Palisades, NY, USA, [15]Department of Geology, Lund University, Lund, Sweden, [16]Institute for Marine Sciences, National Research Council, Bologna, Italy, [17]Geology Department, University of Namibia, Windhoek, Namibia, [18]School of Environmental Science and Technology, Gwangju Institute of Science and Technology, Gwangju, South Korea, [19]CEOAS, Oregon State University, Corvallis, OR, USA, [20]Department of Geosciences, Penn State University, State College, PA, USA, [21]Ocean College, Zhejiang University, Zhoushan, China, [22]Department of Physics, Astronomy & Geosciences, Towson University, Towson, MD, USA, [23]Department of Earth Sciences, University of Oxford, Oxford, UK, [24]Department of Geology, Utah State University, Logan, UT, USA, [25]Department of Geoscience, University of Calgary, Calgary, AB, Canada, [26]Department of Earth and Planetary Sciences, University of Tennessee, Knoxville, TN, USA, [27]Geology Department, University of Namibia, Keetmanshoop, Namibia, [28]Department of Geology, Northwest University, Xi'an, China, [29]School of Environmental Sciences, University of Hull, Hull, UK

Abstract Valdivia Bank (VB) is a Late Cretaceous oceanic plateau formed by volcanism from the Tristan-Gough hotspot at the Mid-Atlantic Ridge (MAR). To better understand its origin and evolution, magnetic data were used to generate a magnetic anomaly grid, which was inverted to determine crustal magnetization. The magnetization model reveals quasi-linear polarity zones crossing the plateau and following expected MAR paleo-locations, implying formation by seafloor spreading over ~4 Myr during the formation of anomalies C34n-C33r. Paleomagnetism and biostratigraphy data from International Ocean Discovery Program Expedition 391 confirm the magnetic interpretation. Anomaly C33r is split into two negative bands, likely by a westward ridge jump. One of these negative anomalies coincides with deep rift valleys, indicating their age and mechanism of formation. These findings imply that VB originated by seafloor spreading-type volcanism during a plate reorganization, not from a vertical stack of lava flows as expected for a large volcano.

Plain Language Summary Oceanic plateaus are large, elevated underwater features commonly formed from volcanic material from a hotspot. Valdivia Bank is a Late Cretaceous oceanic plateau in the southeast Atlantic Ocean formed by volcanism from the Tristan-Gough hotspot near the Mid-Atlantic Ridge. The origin and evolution of Valdivia Bank is poorly defined, but new magnetic data suggests the edifice originated through ridge-centered volcanism, with lateral accretion of crust. This is unlike the evolution of a massive volcano, which would be expected to create a vertical stack of lava flows. Magnetic inversion modeling suggests the plateau was formed by seafloor spreading during the formation of anomalies C34n-C33r, with the plateau becoming younger from east to west, rather than north-south as predicted by some hotspot models. Results from International Ocean Discovery Program Expedition 391 paleomagnetism and biostratigraphy confirm the anomaly interpretation.

Key Points:

- Valdivia Bank is characterized by quasi-linear magnetic anomalies that are parallel to the inferred paleo-Mid-Atlantic Ridge
- Magnetic anomalies imply that the plateau becomes younger E-W consistent with formation via seafloor spreading during anomalies C34n-C33r
- Rift valleys, division of C33r, and anomaly curvature imply complex ridge tectonics and a ridge jump

Supporting Information:

Supporting Information may be found in the online version of this article.

Correspondence to:

S. Thoram,
harsha.thoram@gmail.com

Citation:

Thoram, S., Sager, W. W., Gaastra, K., Tikoo, S. M., Carvallo, C., Avery, A., et al. (2023). Nature and origin of magnetic lineations within Valdivia Bank: Ocean plateau formation by complex seafloor spreading. *Geophysical Research Letters*, *50*, e2023GL103415. https://doi.org/10.1029/2023GL103415

Received 1 MAR 2023
Accepted 11 MAY 2023

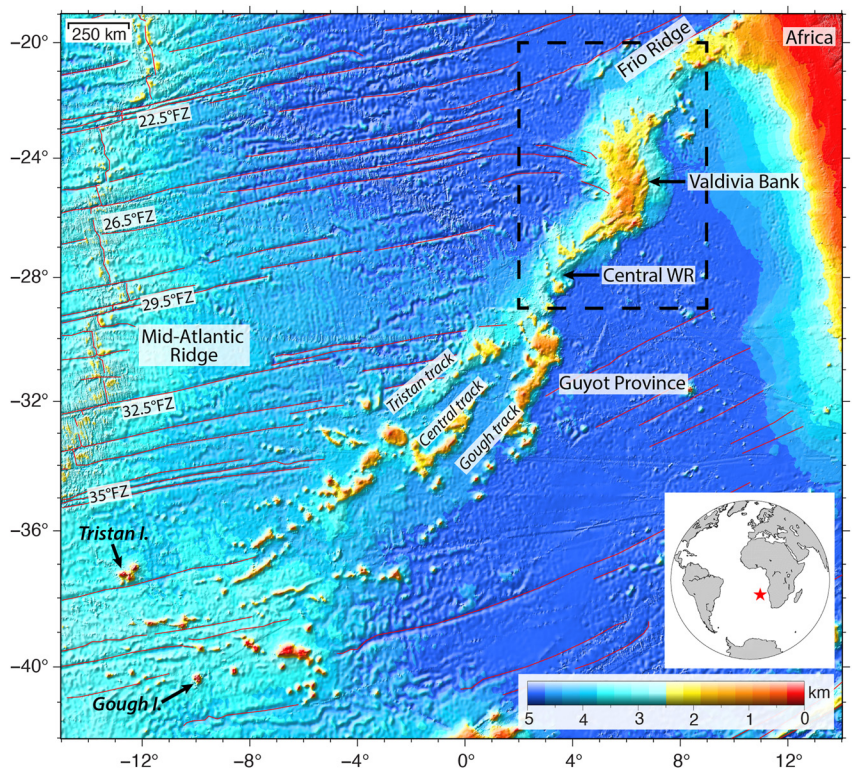

Figure 1. Walvis Ridge bathymetry and feature names. The extent of the study area is indicated by the dashed box. Red lines are fracture zones (Sager et al., 2021). Background is SRTM15+ predicted bathymetry (Tozer et al., 2019). Inset shows the location of Walvis Ridge relative to the South Atlantic.

1. Introduction

Oceanic plateaus are enormous basaltic constructs widely thought to have formed by massive eruptions due to an upwelling mantle plume head (Coffin & Eldholm, 1994; Duncan & Richards, 1991; Richards et al., 1989). An alternative hypothesis explains these eruptions as originating from melting of fertile mantle escaping through cracks in lithospheric plates (Anderson et al., 1992; Foulger, 2007; Saunders et al., 2005). Originally, a hotspot was envisioned to result from a narrow, vertical thermal plume transiting the mantle with little influence from plate boundaries (Morgan, 1971; Wilson, 1965). However, researchers have noted that oceanic plateaus commonly form at spreading ridges and triple junctions, suggesting a strong link between ridge and hotspot volcanism (Sager et al., 2019; Sager & Foulger, 2005; Whittaker et al., 2015). Nevertheless, the origin and tectonic evolution of most oceanic plateaus remains enigmatic due to their enormous size and remote locations in the ocean, often resulting in sparse geological and geophysical data coverage.

Magnetic anomaly patterns can establish the age of oceanic crust (Gee & Kent, 2007) and allow for the tectonic history of an oceanic plateau to be constructed (e.g., Huang et al., 2018, 2021; Sager et al., 2019). Unfortunately, many oceanic plateaus were formed during the Cretaceous Normal Superchron (CNS) (Coffin & Eldholm, 1994), a ~35 Myr period (121-83 Ma; this and other anomaly ages from Ogg, 2020) during which the magnetic field did not reverse polarity. Seafloor formed during this period has no correlatable patterns of magnetic anomalies, making it difficult to study tectonic evolution using magnetic lineations.

Valdivia Bank (VB) is an oceanic plateau offshore of Namibia in the southeast Atlantic Ocean that is part of the Walvis Ridge large igneous province (LIP) (Figure 1). VB formed at the Mid-Atlantic Ridge (MAR) near the end of the CNS (O'Connor & Duncan, 1990). This timing makes it possible to identify Late Cretaceous magnetic anomalies (C34n-C33n) over VB, revealing important clues about its evolution. Magnetic surveys in the South Atlantic are rare and only a few have surveyed in the vicinity of VB (Pérez-Díaz & Eagles, 2017; Thoram et al., 2019) since the pioneering compilation of Cande et al. (1988).

An extensive magnetic survey was conducted over VB onboard R/V *Thomas G. Thompson* during cruises TN373 and TN374 (2019–2020) collecting ~10,730 km of new data (Figure 2). Combining the new data set with previously available data, we constructed a magnetic anomaly map and performed inverse modeling to determine the crustal magnetization. Paleomagnetic and biostratigraphic data from International Ocean Discovery Program (IODP) Expedition 391 drill sites verify the magnetic model. The results indicate that VB becomes younger from east to west, consistent with formation at the MAR.

1.1. Geologic Setting

Walvis Ridge is considered to be the volcanic track of the Tristan-Gough hotspot, erupted on the African plate as the South Atlantic opened (O'Connor & Duncan, 1990; O'Connor & Jokat, 2015). Although the age progression along the volcanic track is highly consistent (Homrighausen et al., 2019), Walvis Ridge has a complex morphology that changes character along its length. It begins as a narrow ridge near the continental margin, includes an oceanic plateau (VB) at nearly right angle to the ridge trend, changes to a series of small volcanic ridges, and splits into two (possibly three) sub-parallel seamount chains, two of which extend to the active volcanic islands of Tristan and Gough (Figures 1 and 2). The change in morphology is hypothesized to be the result of interaction of the hotspot with the MAR (O'Connor & Duncan, 1990; O'Connor & Jokat, 2015), but this process is still not well understood.

During the Late Cretaceous, while the Tristan-Gough hotspot was at the MAR, volcanism erupted on both the African and South American plates forming older Walvis Ridge, including VB, and Rio Grande Rise, a conjugate oceanic plateau on the South American plate (O'Connor & Duncan, 1990). At ~60–70 Ma, the spreading axis and hotspot separated, with the latter moving eastward beneath the African plate, resulting in intraplate volcanism (O'Connor & Duncan, 1990). Subsequently the hotspot formed two or three linear seamount chains (O'Connor & Jokat, 2015).

Several attempts have been made to explain WR by a model using one or more hotspots following the ridge (Doubrovine et al., 2012; Duncan, 1981; O'Connor & Le Roex, 1992; Torsvik et al., 2008), but none adequately account for the complex morphology. A reorganization of the MAR occurred in the South Atlantic during the Late Cretaceous, resulting in changes in spreading direction and formation of a microplate between VB and Rio Grande Rise (Sager et al., 2021). WR tectonic complexity is explained by a reorganization of the MAR in which a long-offset right-lateral transform fault located north of WR at anomaly C34n (83.7 Ma), migrated southward and split into multiple, smaller-offset transforms by anomaly C30n (66.4 Ma). Discontinuities in magnetic lineation sequences suggested that a microplate formed during this reorganization (Sager et al., 2021; Thoram et al., 2019), which was eventually captured by the South American plate. This plate reorganization and microplate formation might have had a significant impact on the evolution of VB but has been poorly understood due to sparse magnetic anomaly coverage. In addition, two prominent rift grabens are observed on the east and southwest flanks of VB (Contreras et al., 2022). The origin and timing of these rifts are unknown and magnetic anomaly patterns may reveal important clues of their origins.

2. Data and Methods

2.1. Magnetic Anomaly Map

Magnetic measurements from a total of 28 cruises spanning 56 years (1963–2019) were compiled for a magnetic anomaly grid encompassing VB (Figure 2; Table S1 in Supporting Information S1). The combined data set amounts to ~37,610 km of track length. Twenty-six of these surveys were acquired from the National Center for Environmental Information (NCEI) database, while the remaining two surveys (TN-373, TN-374) were recently collected. These latter two cruises collected $>10^6$ data points in a pattern of 25 transects (~10,731 km) across VB and nearby Walvis Ridge (Figure 2).

To obtain magnetic anomalies caused by the crustal field, the Earth's main core field was subtracted from the total field using the 13th generation International Geomagnetic Reference Field (IGRF-13; Alken et al., 2021). The resulting anomalies were processed to remove noise, such as spikes or offsets caused by technical issues or disturbances from external factors (e.g., magnetic storms). After noise removal, the data were checked for systematic errors such as drift or offset by analyzing crossover errors (COE), which are data misfits at track crossings. When merging data spanning several decades, the observed data from different surveys often do not agree at track intersections for reasons such as navigation errors, resulting in large COE. Correcting COE improves grid accuracy and can significantly reduce artificial noise and data artifacts. COE analysis was done using the *x2sys* package of GMT 6 software (Wessel et al., 2019) following a procedure similar to that outlined in Huang et al. (2021).

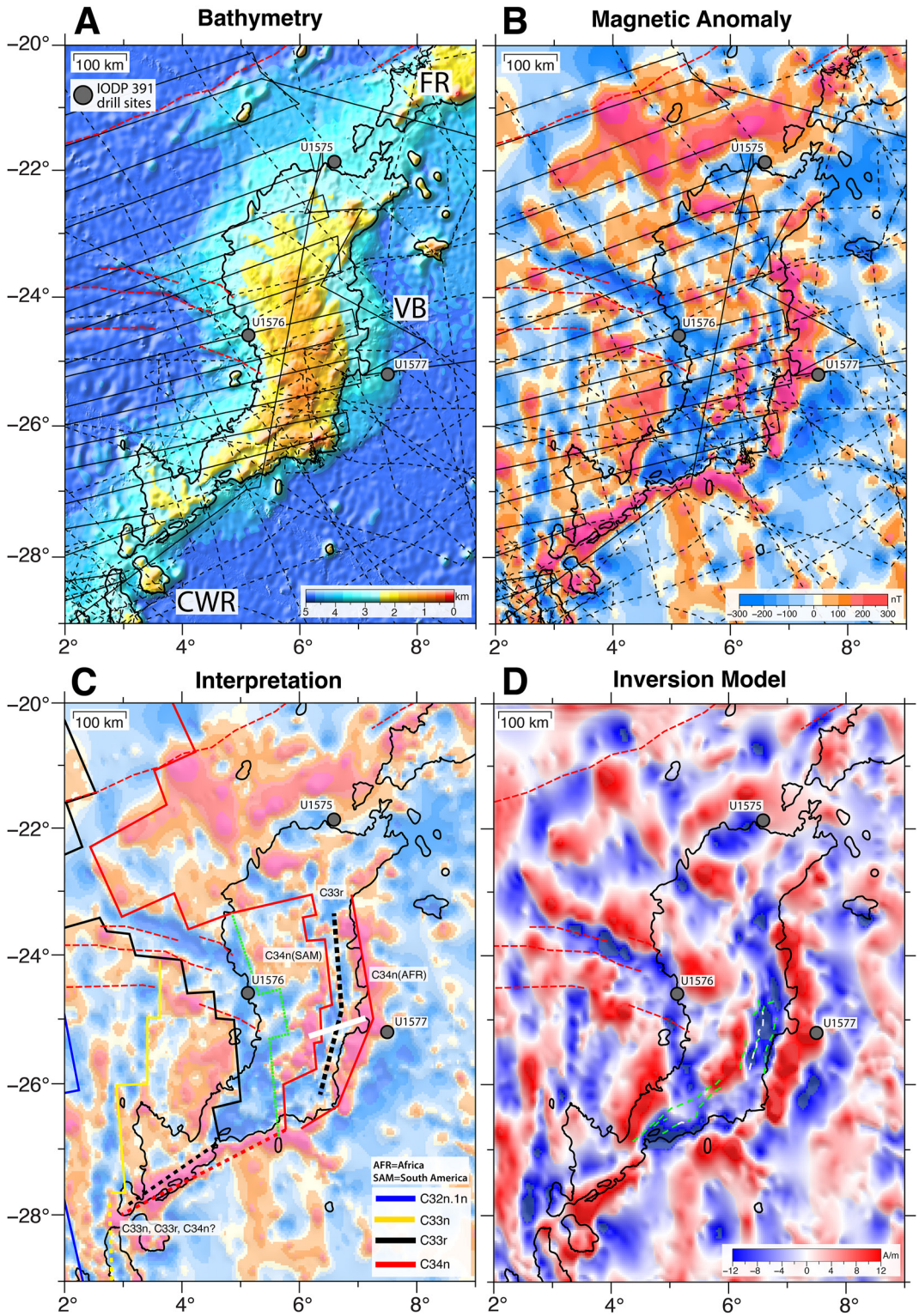

Figure 2.

Only four of the magnetic surveys were navigated with the Global Positioning Satellite (GPS) system, while the rest were surveyed using older, less accurate navigation systems. Older data were merged carefully to generate a coherent magnetic anomaly data set using GPS-navigated data as a "backbone" and adjusting other data to the better-navigated data (see Huang et al., 2021). The combined magnetic anomaly data were averaged within 2 x 2

arc min cells using the GMT routine *blockmean* to avoid spatial aliasing and to average redundant data. The data were gridded using the GMT routine *surface*, using grid spacing of 2 arc min and a tension factor of 0.25 to generate a magnetic anomaly grid (Figure 2).

2.2. Inverse Magnetic Modeling

Magnetic inversion modeling was performed using the method of Parker and Huestis (1974) (Figure 2). This method is a Fourier-domain magnetization inversion approach that solves for lateral variation in crustal magnetization with a magnetic source layer of constant thickness following the topography. This modeling mostly removes the effect of topography on magnetic anomaly data and gives an estimate of magnetization strength and sign. Apropos to this study, this modeling removes the skewness inherent in magnetic anomaly data, allowing less ambiguous determination of crustal magnetic polarity boundaries.

The model requires inputs of magnetic field direction for the ambient field and crustal magnetization. The former was calculated using IGRF-13 (Alken et al., 2021). Crustal magnetization is assumed to be entirely remanent because oceanic basalt samples typically have remanent magnetizations an order of magnitude stronger than the induced magnetization (Harrison et al., 1975). Remanent declination and inclination values of −6° and −42.9° were estimated from the ∼80 Ma Cretaceous paleomagnetic pole for Africa (Torsvik et al., 2012). Magnetic anomalies over oceanic crust are known to be generated primarily from the upper crust and many marine magnetic modeling studies (e.g., Gee & Kent, 2007) assume a thin source layer (∼0.5–1 km). However, gravity inversion over VB revealed the crustal thickness to be ∼3 times that of normal oceanic crust (Graça et al., 2019). Hence a magnetic source layer thickness of 3 km was used for the model, similar to magnetic inversions from other oceanic plateaus (Huang et al., 2018; Sager et al., 2019). This difference mainly affects the magnetization strength but not polarity boundaries. The top of the source layer was set at the sediment-basement interface, calculated by subtracting sediment thickness determined from the NCEI GlobSed model (Straume et al., 2019) from the bathymetry grid.

2.3. IODP 391 Drilling at VB

IODP Expedition 391 cored into igneous rock on the north, west, and south flanks of VB at Sites U1575, U1576, and U1577, respectively (Sager et al., 2022). Sites U1576 and U1577 were sited in part to test the magnetic anomaly interpretation, with the former located on a negative magnetic anomaly and the latter on a positive anomaly. Bio- and magnetostratigraphic analyses were performed on recovered cores to determine age and magnetic polarity (Sager et al., 2022; Text S1 and S2 in Supporting Information S1).

3. Results

The ages magnetic anomalies were taken from the magnetic reversal time scale of Ogg (2020). Following the convention of Cande et al. (1988), all anomaly ages for C34n to C30n correspond the young end of the normal polarity interval (e.g., C30n), except for anomaly C33r, which corresponds to the young end of a long-reversed polarity interval (Figure S1 in Supporting Information S1). The corresponding ages discussed in the text are C34n (83.7 Ma), C33r (79.9 Ma), C33n (74.2 Ma), C32n.1n (71.5 Ma), and C30n (66.4 Ma).

3.1. IODP Core Data

Calcareous nannofossil and foraminifera biostratigraphy data reveal that the oldest sediments at all three sites are lower Campanian stage or older. The Campanian begins at the end of anomaly C34n (CNS) and contains two long periods of constant magnetic polarity, C33r (reversed) and C33n (normal) (Figure S1 in Supporting Information S1). Paleomagnetic measurements of igneous samples from Sites U1575 and U1577 have negative inclinations, implying normal polarity in the southern hemisphere, whereas those from Site U1576 have positive

Figure 2. Geophysical data maps for VB: (a) Bathymetry, (b) magnetic anomaly map, (c) anomaly interpretation and (d) calculated magnetization map using uniform-thickness layer magnetic inversion model (Parker & Huestis, 1974). Bathymetry background is SRTM15+ predicted bathymetry (Tozer et al., 2019). Black contour in all maps is the 3,000 m isobath. Solid black lines in A, B show tracks of newly acquired magnetic data during cruises TN373 and TN374. Dashed lines are older magnetic tracks from the NCEI database. Gray circles show the location of IODP 391 drill sites. Dashed red lines shows the fracture zones. Colored isochron lines correspond to reversals (polarity block edges) but they are labeled by corresponding polarity intervals. Dashed black line in panel C shows the narrow band of anomaly C33r that is separated from the main anomaly C33r on the western flank. Dashed green line shows the older end of the C34n block transferred from the South American plate. Thick white line shows the location of seismic profile VB07 shown in Figure S3 in Supporting Information S1. Dashed green and white lines in Panel D show the locations of rift-bounding faults identified in Contreras et al. (2022). VB = Valdivia Bank, CWR = Central Walvis Ridge, FR = Frio Ridge, AFR = Africa, SAM = South America.

inclinations, implying reversed polarity. Thick chalk sequences were recovered above basement at Sites U1576 and U1577 providing magnetic stratigraphy context. Basal sediments from both holes show a long-reversed polarity chron that is interpreted as C33r (Sager et al., 2022; Figures S4 and S5 in Supporting Information S1) because this is the only reversed period during the early Campanian. At Site U1576, the C33r sediment chronozone is contiguous with reversed polarity igneous basement. The transition to C33n (79.9 Ma) is ∼3–6 m above the basement surface (Figure S4 in Supporting Information S1). At Site U1577, the transition from C34n to C33r occurs in chalk ∼7 m above the basement surface. Biostratigraphy indicates that basal sedimentary rocks at this site are earliest Campanian and possibly Turonian, consistent with C34n (Sager et al., 2022; Figure S5 in Supporting Information S1). Microfossil biostratigraphy indicates a sedimentation rate of ∼14–16 m/Ma at both sites. The implication is that basement at Site U1576 formed during C33r, ∼0.3 Ma prior to the start of chron C33n (i.e., ∼80.2 Ma). Basement at Site U1577 formed during C34n, ∼0.5 Ma prior to the end of that chron (i.e., ∼84.2 Ma).

3.2. Anomaly Map Interpretation

The study area spans the region between the 22.5°S fracture zone (FZ) and 30°S FZ (latitudes at the MAR) and contains VB and the central WR immediately to the west. The gridding algorithm produced well-constrained anomaly patterns in places with dense data coverage, but rounded and ambiguous anomaly patterns in regions with limited data coverage. Track coverage has been significantly improved over VB and central WR, owing to the new magnetic surveys conducted for this study. In contrast, coverage is poor in the region east of VB, over the area of 26°–29°S, 1°–6°E, with only a few tracks traversing the area, resulting in poorly defined anomalies.

The new magnetic anomaly map reveals four bands of quasi-linear magnetic anomalies (two normal and two reversed), that traverse VB and have ∼N-S trends (Figure 2). The most striking is a curved negative anomaly along the VB western flank (Figure 2), which has been interpreted as C33r (Cande et al., 1988; Thoram et al., 2019). This interpretation is supported by bio- and magneto-stratigraphic ages from IODP Site U1576 (Sager et al., 2022; Figure S4 in Supporting Information S1). Under symmetrical spreading conditions, the expected C33r anomaly on one plate is a linear negative band with a trend of N26°W and width of ∼170 km, which is observed in the spreading corridors north of the Rio Grande-Florianopolis FZ (22.5°S at the MAR) and south of the 32.5° FZ (Figure S2 in Supporting Information S1). However, C33r on the west flank of VB is curved and has irregular width ranging from 30 to 170 km. Over the northwest flank of VB, where the C33r curve is greatest, the anomaly width ranges from 30 to 70 km. Farther south, the C33r anomaly reaches a uniform width of 110–120 km between 24°S and 26°S, after which it widens to 170 km and ends over southern VB (5°E, 26.5°S; Figure 2). The width of the C33r anomaly at its middle (24°S–26°S) is ∼50 km less than the expected width. Thus, the missing part(s) of the anomaly must be elsewhere. Notably, at this latitude, another narrow negative band is observed over the eastern flank of VB (6.5°E, 25°S; Figure 2). This band has a ∼N-S trend and a width of ∼60 km. Over southern VB, this eastern anomaly joins with the western negative anomaly in a v-shape, where the anomaly has a width of ∼170 km. The anomalies over the eastern flank and the SE flank coincide with fault scarps mapped in seismic and bathymetry data that bound the rift valleys (Contreras et al., 2022) (Figure 2, Figure S3 in Supporting Information S1).

A strong linear positive anomaly is observed along the eastern flank of VB (7°E, 26°S). This anomaly trends ∼N-S, parallel to the bathymetry contours from 23°S to 29°S, but at 29°S, it bends by ∼110° and trends southwest between 7°E to 4°E along the WR. IODP Site U1577 was drilled into this normal polarity band and bio- and magneto-stratigraphic data indicate normal polarity with a basement age of ∼84.1 Ma, suggesting formation near the end of the CNS, that is, C34n (Sager et al., 2022; Figure S5 in Supporting Information S1).

The wide positive anomaly band immediately to the west of C33r is interpreted as anomaly C33n. The expected width of anomaly C33n at this location is ∼200 km. However only part of C33n is present. It narrows southward from ∼170 km at 24°S to ∼90 km at 28°S. Farther south, it is absent (over central WR). To the west of C33n, anomalies C30n and C32n.1n (Figure S1 in Supporting Information S1) are two narrow positive anomaly bands with a narrow negative band separating them (Figure S2 in Supporting Information S1). Anomalies C33n-C30n all trend ∼N15°W perpendicular to, and terminate at, the curved FZ at 26.5°S, west of VB. To the south of VB, in the central WR corridor, anomalies C32n.1n-C30n terminate at the 29.5°FZ (latitude at MAR), where they are offset by ∼75 km. Anomalies C34n-C33n are missing south of 28°S but are found further south of 33°S (Thoram et al., 2019).

4. Discussion

4.1. Formation and Evolution of VB

The magnetic anomaly map reveals VB to be cross-cut by quasi-linear magnetic anomalies that trend ~N-S, roughly parallel the paleo-MAR, implying that the anomalies are related to more-of-less E-W seafloor spreading (Figure 2). Several studies have shown that oceanic plateaus formed at spreading ridges (such as Tamu Massif, Rio Grande Rise, and Azores) can record magnetic lineations (Cande et al., 1988; Gente et al., 2003; Sager et al., 2019). Based on magnetic studies of Tamu Massif, Sager et al. (2019) proposed that oceanic plateau formation at spreading ridges can occur by voluminous ridge-centered volcanism, resulting in the preservation of magnetic lineations within plateau crust, rather than eruption on top of pre-existing crust by a series of lava flows. The magnetic anomaly map implies that similar ridge-centered volcanism formed VB.

Based on the magnetization inversion results, VB contains four polarity bands: wider positive and negative magnetization zones on the east and west flanks, respectively, surrounding narrow positive and negative bands near the center (Figure 2). IODP Expedition 391 core data agree with the identification of two of these polarity bands: C33r on the west flank and C34n on the east flank. In their synthesis of South Atlantic magnetic anomalies, Cande et al. (1988) did not identify C34n near VB. In a prior study, we identified C34n as the positive anomaly at the western edge of the curved C33r (Thoram et al., 2019). Here we follow the drilling results and identify C34n as the strong positive anomaly on the distal east flank of VB. The high amplitude of this anomaly is consistent with C34n being an anomaly peak caused by the contrast in polarity at the end of the CNS (Figure S1 in Supporting Information S1). This interpretation poses a problem—what are the anomalies in between C33r on the west flank and C34n on the east flank (Figure 2)?

Unlike other nearby magnetic anomalies, C33r over western VB has a curved shape. A major plate reorganization occurred in the South Atlantic during Late Cretaceous between the fracture zones at 22°S and 35.5°S, beginning prior to 84 Ma and ending at ~66 Ma (Sager et al., 2021). This plate reorganization was accompanied by microplate formation and ridge propagation between VB and Rio Grande Rise that resulted in the transfer of crust between the African and South American plates (Sager et al., 2021). When a propagating ridge transfers seafloor from one plate to another, the originally ridge-parallel isochrons in a zone between the growing and failed rifts can be reoriented to trends oblique to both the ridge and spreading direction (McKenzie, 1986). This mechanism likely caused the C33r anomaly band to be curved and trend oblique to the African-South American plate spreading direction. Another mechanism that could explain the curved C33r anomaly is microplate rotation, during which the two C33r stripes may have been forming simultaneously around the boundaries of the microplate. Anomaly widths suggest that the entire C33r is not present on the west VB flank and is short by ~50 km from the expected width (Thoram, 2021). Importantly, a narrow ~N-S trending negative magnetic band is mapped over the eastern flank in the same latitudes with a width of ~50 km. Anomaly C33r over the eastern flank of Rio Grande Rise appears to have the expected width (Cande et al., 1988). Thus, crust missing from C33r on the west flank of VB is not on the South American plate. These observations imply that the narrow negative band over the eastern summit of VB is the missing anomaly C33r crust. This suggests that a tectonic event must have bifurcated the negative anomaly band of C33r into two negative anomaly bands—a wide anomaly band over the western flank and a narrow negative band atop the eastern flank. Notably, the rift valley over the VB east flank coincides exactly with the narrow negative anomaly band. This correspondence suggests that the rift is an abandoned spreading center, left behind by an westward ridge jump.

A narrow positive band separates these two C33r negative anomaly bands. Based on anomaly correlations, Thoram et al. (2019) interpreted this positive band to be anomaly C34n. However, this positive anomaly can have two possible origins. Either this anomaly is part of the CNS or it could be part of anomaly C33r that was remagnetized later due to secondary volcanism known to have occurred at VB (Homrighausen et al., 2018). If the crust was remagnetized or buried by lavas of C33n age or younger, the total width of anomaly C33r generated would be greater than the expected width for this part of the South Atlantic and is therefore unlikely. Hence this anomaly band is likely a sliver of the CNS. Furthermore, the strong positive anomaly bounding VB on the east, which we interpret as C34n is consistent with the igneous basement age inferred for Site 1577 (Sager et al., 2022; Figure S5 in Supporting Information S1). Based on reconstruction of the magnetic anomalies, Sager et al. (2021) suggested that CNS crust exists between VB and Rio Grande Rise. This implies that C34n crust within VB came from the South American plate, and the anomaly patterns imply that this crust was incorporated into VB via the westward

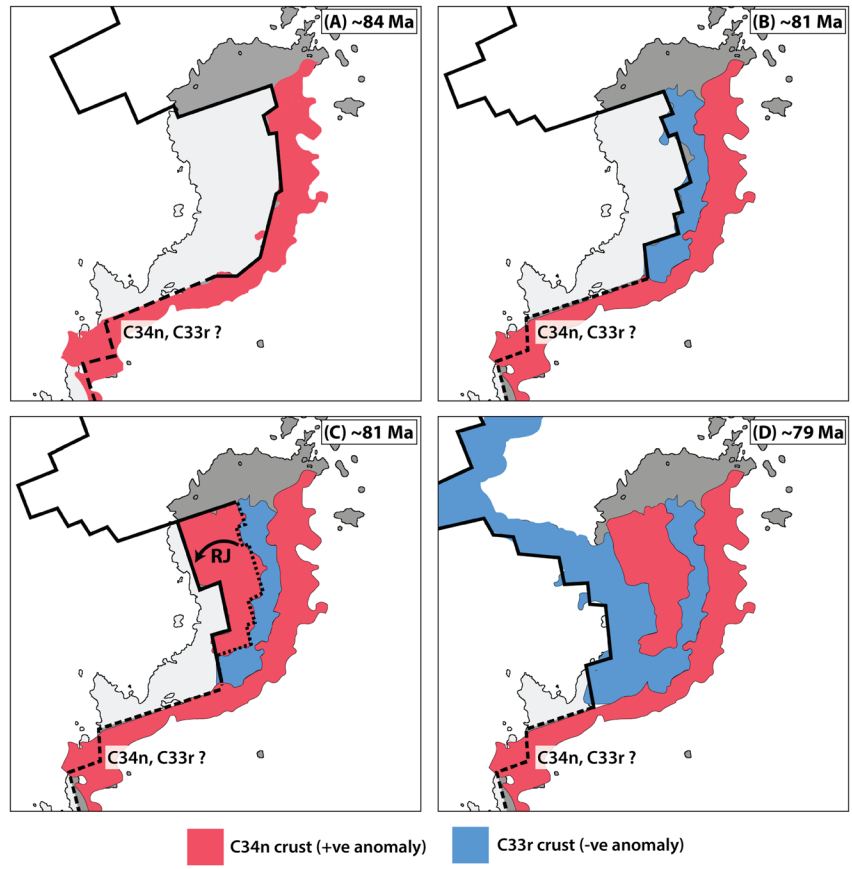

Figure 3. Tectonic sketch showing the evolution of VB. The 3,000 m isobath is shown for reference. Dark gray region is the region of VB that has already formed at the reconstructed time. Light gray region shows the part of VB that has not yet formed at that time. Thick black line shows the location of the MAR at a particular time. Dashed black line indicates the MAR where it cannot be inferred either due to complex anomaly patterns or missing crust. (a) At ~84 Ma—Eastern flank of VB forms during C34n (CNS). (b) At ~81 Ma—Part of C33r formed atop eastern flank, (c) After ~81 Ma, a ridge jump (RJ) incorporated CNS crust into VB. Dotted line shows the abandoned spreading center (d) At ~79 Ma—completion of VB during the remainder of C33r.

ridge jump that resulted in the bifurcation of negative anomaly C33r. Ridge jumps occur frequently during plate reorganizations, often resulting from a change in spreading direction (Nakanishi et al., 1999; Sager et al., 2019).

In summary, our anomaly interpretation over VB, supported by IODP Expedition 391 basement ages from bio- and magnetostratigraphic analysis, suggests that VB formed during at the end of the CNS, recording anomaly C34n and C33r. This suggests that VB was built by eruptions along the MAR over a period of ~4 Myr, the time span between estimated basement ages at Sites U1576 and U1577. Near the beginning of C33r, the hotspot was at the MAR and eruptions formed the eastern flank of VB (Figure 3a). After forming one-third of the total C33r crust (Figure 3b), a westward ridge jump incorporated a narrow slice of CNS crust from the South American plate (Figure 3c). Subsequent recording of the remainder of C33r resulted in the bifurcated negative anomaly bracketing the positive anomaly over central VB (Figure 3d). Ridge propagation at the edge of a microplate between VB and Rio Grande Rise caused the western C33r to be curved (Figure 3d). After forming VB, ridge propagation continued southward into central WR, transferring crust from the African to the South American plate, as evidenced by missing anomalies C34n-C33n over Central WR (Thoram et al., 2019) and repetition of anomalies C34n-C33n to the south of Rio Grande Rise (Cande et al., 1988). The ridge propagation and plate reorganization ended at the 35° FZ and normal spreading was restored in South Atlantic by C30n (66.4 Ma; Sager et al., 2021).

These findings indicate that VB becomes younger E-W, rather than N-S as predicted by several hotspot models (Duncan, 1981; O'Connor & le Roex, 1992; Torsvik et al., 2008; Doubrovine et al., 2012). However, the E-W progression was disrupted by a ridge jump which captured a narrow band of South American crust. Furthermore,

the narrow C33r band atop the eastern flank exactly coincides with a prominent rift valley that was mapped in seismic and bathymetry data (Contreras et al., 2022; Figure S3 in Supporting Information S1). Similar rifts are found within Rio Grande Rise (Gamboa & Rabinowitz, 1984) and are probably related to the VB rifts (Sager et al., 2021). Deep rift valleys have been observed near the boundaries of other microplates (e.g., Easter microplate) caused due to faulting and complex deformation (Naar & Hey, 1991; Searle et al., 1989).

5. Conclusion

The improved anomaly grid over VB shows four quasi-linear bands of alternating that parallel the paleo-MAR and surrounding seafloor magnetic lineations, implying that they were formed by seafloor spreading. These anomalies are interpreted as C34n and a split anomaly C33r. Biostratigraphic and paleomagnetic data from IODP Expedition 391 support these anomaly interpretations. The data imply that VB was formed by eruptions at the MAR over a ∼4 Myr time span, mainly during anomaly C33r. The lineation pattern suggests VB becomes younger E-W, rather than the ∼N-S age progression suggested by hotspot models. VB crust was formed by seafloor spreading, with lateral accretion of crust, rather than the stacking of lava flows atop pre-existing crust by a massive volcano.

At around 83.7 Ma (C34n), the eastern flank of VB was formed at the MAR. Subsequently, negative polarity crust formed recording anomaly C33r. After about one-third of this anomaly was formed (around 82.4 Ma), a westward ridge jump occurred slicing off a narrow band of positive CNS crust from the South American plate and capturing it as part of VB. Thereafter, the remainder of the C33r crust formed the west flank of VB, although MAR reorganization caused the C33r anomaly band to curve. The formation of VB was completed by the end of chron C33r. The negative anomaly band atop the eastern flank of VB exactly coincides with a deep rift valley in bathymetry and seismic data. This coincidence indicates that the rift formed via spreading during C33r. This rift valley is interpreted as an abandoned spreading center.

Conflict of Interest

The authors declare no conflicts of interest relevant to this study.

Data Availability Statement

All the magnetic data used in this study, including data from cruises TN-373 and TN-374 are archived on the Zenodo database (https://doi.org/10.5281/zenodo.7662198). The new magnetic data will eventually be added to the NCEI marine geophysics database. The 1-min resolution VB magnetic anomaly grid and magnetization grid generated in this study are also archived on the Zenodo database (https://doi.org/10.5281/zenodo.7662198).

Acknowledgments
We thank the captains and crews of R/V *Thomas G. Thompson* (TN-373, TN-374) and D/V *JOIDES resolution* (IODP Expedition 391) for their assistance in collecting data. We especially appreciate the hard work and efficiency of the IODP technical staff. ST and WS were supported by NSF Grant OCE-1832197, which also supported cruises TN-373 and TN-374. ST, WS, KG, SMT, and AA were supported by the US Science Support Program for Expedition 391 research. CC and AVD were supported by ECORD. YH was supported by National Natural Science Foundation of China Grant 42006056. We thank Doug Wilson and an anonymous reviewer for constructive comments that significantly improved this paper.

References

Alken, P., Thébault, E., Beggan, C. D., Amit, H., Aubert, J., Baerenzung, J., et al. (2021). International geomagnetic reference field: The thirteenth generation. *Earth Planets and Space*, *73*(1), 1–25. https://doi.org/10.1186/s40623-020-01288-x

Anderson, D. L., Tanimoto, T., & Zhang, Y.-S. (1992). Plate tectonics and hotspots: The third dimension. *Science*, *256*(5064), 1645–1651. https://doi.org/10.1126/science.256.5064.1645

Cande, S. C., LaBrecque, J. L., & Haxby, W. F. (1988). Plate kinematics of the South Atlantic: Chron C34 to present. *Journal of Geophysical Research*, *93*(B11), 13479–13492. https://doi.org/10.1029/JB093iB11p13479

Coffin, M. F., & Eldholm, O. (1994). Large igneous provinces: Crustal structure, dimensions, and external consequences. *Reviews of Geophysics*, *32*(1), 1–36. https://doi.org/10.1029/93RG02508

Contreras, E., García, P. J., Sager, W. W., Thoram, S., Hoernle, K., Sarralde, R., & Zhou, H. (2022). Bathymetry of Valdivia Bank, Walvis Ridge, South Atlantic Ocean: Implications for structure and geologic history of a hot spot plateau. *Geochemistry, Geophysics, Geosystems*, *23*(11), e2022GC010624. https://doi.org/10.1029/2022GC010624

Doubrovine, P., Steinberger, B., & Torsvik, T. (2012). Absolute plate motions in a reference frame defined by moving hot spots in the Pacific, Atlantic, and Indian oceans. *Journal of Geophysical Research*, *117*(B9), B09101. https://doi.org/10.1029/2011JB009072

Duncan, R. A. (1981). Hotspots in the southern oceans—An absolute frame of reference for motion of the Gondwana continents. *Tectonophysics*, *74*(1–2), 29–42. https://doi.org/10.1016/0040-1951(81)90126-8

Duncan, R. A., & Richards, M. A. (1991). Hotspots, mantle plumes, flood basalts, and true polar wander. *Reviews of Geophysics*, *29*(1), 31–50. https://doi.org/10.1029/90RG02372

Foulger, G. R. (2007). The "Plate" model for the genesis of melting anomalies. *Special Papers - Geological Society of America*, *430*, 1–28. https://doi.org/10.1130/2007.2430(01)

Gamboa, L. A. P., & Rabinowitz, P. D. (1984). The evolution of the Rio Grande Rise in the southwest Atlantic Ocean. *Marine Geology*, *58*(1–2), 35–58. https://doi.org/10.1016/0025-3227(84)90115-4

Gee, J. S., & Kent, D. V. (2007). Source of oceanic magnetic anomalies and the geomagnetic polarity time scale. In M. Kono (Ed.), *Treatise on geophysics* (Vol. 5, pp. 455–507). Geomagnetism, Elsevier. https://doi.org/10.1016/B978-044452748-6.00097-3

Gente, P., Dyment, J., Maia, M., & Goslin, J. (2003). Interaction between the Mid-Atlantic Ridge and the Azores hot spot during the last 85 Myr: Emplacement and rifting of the hot spot-derived plateaus. *Geochemistry, Geophysics, Geosystems*, *4*(10), 8514. https://doi.org/10.1029/2003GC000527

Graça, M. C., Kusznir, N., & Stanton, N. S. G. (2019). Crustal thickness mapping of the central South Atlantic and the geodynamic development of the Rio Grande Rise and Walvis Ridge. *Marine and Petroleum Geology*, *101*, 230–242. https://doi.org/10.1016/j.marpetgeo.2018.12.011

Harrison, C. G. A., Jarrard, R. D., Vacquier, V., & Larson, R. L. (1975). Paleomagnetism of Cretaceous Pacific seamounts. *Geophysical Journal of the Royal Astronomical Society*, *42*(3), 859–882. https://doi.org/10.1111/j.1365-246X.1975.tb06455.x

Homrighausen, S., Hoernle, K., Geldmacher, J., Wartho, J.-A., Hauff, F., Portnyagin, M., et al. (2018). Unexpected HIMU-type late-stage volcanism on the Walvis Ridge. *Earth and Planetary Science Letters*, *492*, 251–263. https://doi.org/10.1016/j.epsl.2018.03.049

Homrighausen, S., Hoernle, K., Hauff, F., Wartho, J.-A., van den Bogaard, P., & Garbe-Schönberg, D. (2019). New age and geochemical data from the Walvis Ridge: The temporal and spatial diversity of South Atlantic intraplate volcanism and its possible origin. *Geochimica et Cosmochimica Acta*, *245*, 16–34. https://doi.org/10.1016/j.gca.2018.09.002

Huang, Y., Sager, W. W., Tominaga, M., Greene, J. A., Zhang, J., & Nakanishi, M. (2018). Magnetic anomaly map of Ori Massif and its implications for oceanic plateau formation. *Earth and Planetary Science Letters*, *501*, 46–55. https://doi.org/10.1016/j.epsl.2018.08.029

Huang, Y., Sager, W. W., Zhang, J., Tominaga, M., Greene, J., & Nakanishi, M. (2021). Magnetic anomaly map of Shatsky Rise and its implications for oceanic plateau formation. *Journal of Geophysical Research: Solid Earth*, *126*(2), e2019JB019116. https://doi.org/10.1029/2019JB019116

McKenzie, D. (1986). The geometry of propagating rifts. *Earth and Planetary Science Letters*, *77*(2), 176–186. https://doi.org/10.1016/0012-821X(86)90159-7

Morgan, W. J. (1971). Convection plumes in the lower mantle. *Nature*, *230*(5288), 42–43. https://doi.org/10.1038/230042a0

Naar, D. F., & Hey, R. N. (1991). Tectonic evolution of the Easter microplate. *Journal of Geophysical Research*, *96*(B5), 7961–7993. https://doi.org/10.1029/90JB02398

Nakanishi, M., Sager, W. W., & Klaus, A. (1999). Magnetic lineations within Shatsky Rise, northwest Pacific Ocean: Implications for hot spot-triple junction interaction and oceanic plateau formation. *Journal of Geophysical Research*, *104*(B4), 7539–7556. https://doi.org/10.1029/1999JB900002

O'Connor, J. M., & Duncan, R. A. (1990). Evolution of the Walvis Ridge-Rio Grande Rise hot spot system: Implications for African and South American plate motions over plumes. *Journal of Geophysical Research*, *95*(B11), 17475–17502. https://doi.org/10.1029/JB095iB11p17475

O'Connor, J. M., & Jokat, W. (2015). Tracking the Tristan-Gough mantle plume using discrete chains of intraplate volcanic centers buried in the Walvis Ridge. *Geology*, *43*(8), 715–718. https://doi.org/10.1130/G36767.1

O'Connor, J. M., & le Roex, A. P. (1992). South Atlantic hot spot-plume systems: 1. Distribution of volcanism in time and space. *Earth and Planetary Science Letters*, *113*(3), 343–364. https://doi.org/10.1016/0012-821X(92)90138-L

Ogg, J. G. (2020). Geomagnetic polarity time scale. In F. M. Gradstein, J. G. Ogg, M. D. Schmitz, & G. M. Ogg (Eds.), *Geologic time scale 2020* (pp. 159–192). https://doi.org/10.1016/b978-0-12-824360-2.00005-x

Parker, R. L., & Huestis, S. P. (1974). The inversion of magnetic anomalies in the presence of topography. *Journal of Geophysical Research*, *79*(11), 1587–1593. https://doi.org/10.1029/JB079i011p01587

Pérez-Díaz, L., & Eagles, G. (2017). A new high-resolution seafloor age grid for the South Atlantic. *Geochemistry, Geophysics, Geosystems*, *18*(1), 457–470. https://doi.org/10.1002/2016GC006750

Richards, M. A., Duncan, R. A., & Courtillot, V. E. (1989). Flood basalts and hot-spot tracks: Plume heads and tails. *Science*, *246*(4926), 103–107. https://doi.org/10.1126/science.246.4926.103

Sager, W., Hoernle, K., Höfig, T. W., & the Expedition 391 Scientists (2022). *Expedition 391 preliminary report: Walvis ridge hotspot*. International ocean discovery program. https://doi.org/10.14379/iodp.pr.391.2022

Sager, W. W., & Foulger, G. R. (2005). What built Shatsky Rise, mantle plume or ridge tectonics? *Special Papers - Geological Society of America*, *388*, 721. https://doi.org/10.1130/0-8137-2388-4.721

Sager, W. W., Huang, Y., Tominaga, M., Greene, J. A., Nakanishi, M., & Zhang, J. (2019). Oceanic plateau formation by seafloor spreading implied by Tamu Massif magnetic anomalies. *Nature Geoscience*, *12*(8), 661–666. https://doi.org/10.1038/s41561-019-0390-y

Sager, W. W., Thoram, S., Engfer, D. W., Koppers, A. A. P., & Class, C. (2021). Late Cretaceous ridge reorganization, microplate formation, and the evolution of the Rio Grande Rise-Walvis ridge hot spot twins, South Atlantic Ocean. *Geochemistry, Geophysics, Geosystems*, *22*(3), e2020GC009390. https://doi.org/10.1029/2020GC009390

Saunders, A. D., England, R. W., Reichow, M. K., & White, R. V. (2005). A mantle plume origin for the Siberian traps: Uplift and extension in the west Siberian basin, Russia. *Lithos*, *79*(3–4), 407–424. https://doi.org/10.1016/j.lithos.2004.09.010

Searle, R. C., Rusby, R. I., Engeln, J., Hey, R. N., Zukin, J., Hunter, P. M., et al. (1989). Comprehensive sonar imaging of the Easter microplate. *Nature*, *341*(6244), 701–705. https://doi.org/10.1038/341701a0

Straume, E., Gaina, C., Medvedev, S., Hochmuth, K., Gohl, K., Whittaker, J., et al. (2019). GlobSed: Updated total sediment thickness in the world's oceans. *Geochemistry, Geophysics, Geosystems*, *20*(4), 1756–1772. https://doi.org/10.1029/2018GC008115

Thoram, S. (2021). Tectonic evolution of oceanic plateaus and hotspot-ridge interactions: Walvis Ridge-Rio Grande Rise, South Atlantic, and Tamu Massif, Pacific Ocean. (doctoral dissertation). Retrieved from https://hdl.handle.net/10657/9272

Thoram, S., Sager, W. W., & Jokat, W. (2019). Implications of updated magnetic anomalies for the Late Cretaceous tectonic evolution of Walvis Ridge. *Geophysical Research Letters*, *46*(16), 9474–9482. https://doi.org/10.1029/2019GL083467

Torsvik, T., Muller, R., Voo, R., Steinberger, B., & Gaina, C. (2008). Global plate motion frames: Toward a unified model. *Reviews of Geophysics*, *46*(3), RG3004. https://doi.org/10.1029/2007RG000227

Torsvik, T., Voo, R., Preeden, U., Mac Niocaill, C., Steinberger, B., Doubrovine, P., et al. (2012). Phanerozoic polar wander, palaeogeography and dynamics. *Earth-Science Reviews*, *114*(3–4), 325–368. https://doi.org/10.1016/j.earscirev.2012.06.007

Tozer, B., Sandwell, D. T., Smith, W. H. F., Olson, C., Beale, J. R., & Wessel, P. (2019). Global bathymetry and topography at 15 arc sec: SRTM15+. *Earth and Space Science*, *6*(10), 1847–1864. https://doi.org/10.1029/2019EA000658

Wessel, P., Luis, J. F., Uieda, L., Scharroo, R., Wobbe, F., Smith, W. H. F., & Tian, D. (2019). The generic mapping tools version 6. *Geochemistry, Geophysics, Geosystems*, *20*(11), 5556–5564. https://doi.org/10.1029/2019GC008515

Whittaker, J. M., Afonso, J. C., Masterton, S., Müller, R. D., Wessel, P., Williams, S. E., & Seton, M. (2015). Long-term interaction between mid-ocean ridges and mantle plumes. *Nature Geoscience*, *8*(6), 479–483. https://doi.org/10.1038/ngeo2437

Wilson, J. (1965). A new class of faults and their bearing on continental drift. *Nature*, *207*(4995), 343–347. https://doi.org/10.1038/207343a0

References From the Supporting Information

Meyer, B., Chulliat, A., & Saltus, R. (2017). Derivation and error analysis of the Earth magnetic anomaly grid at 2 arc min resolution version 3 (EMAG2v3). *Geochemistry, Geophysics, Geosystems*, *18*(12), 4522–4537. https://doi.org/10.1002/2017GC007280

Reagan, M. K., Pearce, J. A., Petronotis, K., Almeev, R., Avery, A. A., Carvallo, C., et al. (2015). Expedition 352 methods. *Reagan, MK, Pearce, JA, Petronotis, K., and the Expedition*, *352*. https://doi.org/10.14379/iodp.proc.352.102.2015